Universal behavior of harmonic susceptibilities in type-II superconductors

S. Shatz, A. Shaulov,* and Y. Yeshurun
Department of Physics, Bar-Ilan University, 52100 Ramat-Gan, Israel
(Received 22 February 1993; revised manuscript received 9 July 1993)

Simple analytical expressions are derived for the harmonic susceptibilities in type-II superconductors, using a critical-state model with a general dependence of the critical current upon magnetic field. It is shown that the harmonic susceptibilities are determined by a single parameter, δ, which is a function of the full penetration field of the sample and the applied alternating field. This implies that measurements of harmonic susceptibilities as a function of any experimental variable, in any irreversible type-II superconductor, can be reduced to universal curves that describe the harmonic susceptibilities versus δ. In particular, the maximum values that can be attained by the harmonic susceptibilities are universal constants for irreversible type-II superconductors. Fitting of experimental data to the universal curves provides models for the dependence of the critical current density upon field and temperature. This is demonstrated using data of the third-harmonic response measured in a sintered $YBa_2Cu_3O_{7-\delta}$ sample.

INTRODUCTION

Magnetic measurements using alternating fields have been widely employed in the study of superconductors. Commonly, a linear magnetic behavior is assumed and the material response is studied in terms of the fundamental complex susceptibility $\chi_1=\chi_1'-i\chi_1''$. However, recent studies have shown the importance of the *nonlinear* magnetic behavior of type-II superconductors.[1-5] In such materials, the magnetization induced by an applied sinusoidal field $H_{ac}\sin\omega t$ may be described as a sum of sinusoidal components which oscillate at harmonics of the driving frequency:

$$M(t)=H_{ac}\sum_{n=1}^{\infty}(\chi_n'\sin n\omega t-\chi_n''\cos n\omega t)\ ,$$

where χ_n' and χ_n'' $(n=1,2,3,\ldots)$ are defined as the in-phase and out-of-phase components of the harmonic susceptibilities. Clearly, investigation of materials with a nonlinear magnetic behavior requires the study of harmonic susceptibilities beyond the fundamental susceptibility χ_1.

The first prediction of harmonic susceptibilities in type-II superconductors emerged from the original Bean model of the critical state.[6] This model attributes the harmonic generation to the hysteretic, nonlinear relationship between the magnetization and the external field due to flux pinning. Ishida and Mazaki[7] studied harmonic susceptibilities in a multiconnected superconductor, which they modeled as a multiconnected Josephson network. Recently, various new models have been proposed to explain the nonlinear magnetic behavior of high-temperature superconductors. Jeffries *et al.*[8] investigated magnetic nonlinearity in granular $YBa_2Cu_3O_{7-\delta}$ (YBCO), proposing a model of flux-quantized supercurrent loops with Josephson junctions. Xenikos and Lemberger[4] observed nonlinear magnetic behavior in YBCO crystals and interpreted it as a consequence of the nonlinear magnetoresistance of the crystals near T_c, due to flux creep. Ji *et al.*[2] have extended the Bean model by taking into account the field dependence of the critical current. Using a simplified Kim model, in which the critical current density is inversely proportional to the local field, they derived analytical expressions for the magnetic hysteresis loops. Using these equations, they numerically computed χ_n and compared it with experimental data. Ishida and Goldfarb[3] reported a detailed experimental study of the field and temperature dependence of the harmonic susceptibilities in YBCO ceramics and showed good agreement between the predictions of Ji *et al.* and the experimental data. Although the model of Ji *et al.* has successfully explained a broad range of experimental results, no universal picture on the dependence of the harmonic susceptibilities on the various physical parameters has emerged from this model.

In this paper we derive analytical expressions for the harmonic susceptibilities using the critical-state model with no specific assumption regarding the field dependence of the critical current. Our analysis shows that the harmonic susceptibilities are determined by a single parameter δ which measures the extent of penetration of the applied alternating field into the sample. This result implies that measurements of harmonic susceptibilities as a function of any experimental variable, in any irreversible type-II superconductor, can be reduced to universal curves which describe the harmonic susceptibilities versus δ. A particular result of this analysis is that the maximum values which are attained by the harmonic susceptibilities, as a function of any experimental variable, are universal constants for irreversible type-II superconductors. We illustrate the application of this analysis by fitting experimental data taken in a sintered YBCO sample to a universal curve. In this process we decide upon a suitable model for the dependence of the critical current density on field and temperature.

THEORETICAL ANALYSIS

Our analysis is based on a critical-state model assuming no specific relationship between the critical current

density J and the local magnetic field h. To illustrate the theoretical arguments, consider an infinite superconducting slab in a steady field H_{dc}, parallel to its surface. In order to measure the harmonic susceptibilities, a small alternating field $H_{ac}\sin(\omega t)$ is applied in the same direction. A basic assumption of our analysis is that the alternating field can be considered as a small perturbation to the steady field, i.e., $H_{ac} \ll H_{dc}$. We argue that in this case the flux profile in the regions of the slab affected by the alternating field is approximately linear with a slope $S=\pm 4\pi J(H_{dc})/c$. (Obviously, the whole flux profile need not be linear.) Accordingly, the alternating part of the magnetization becomes a function of a single parameter: the slope S. To prove this point, let us review some basics of the critical-state model.

This model predicts that the magnetic field induces internal currents of a critical density $J(h)$ in a direction determined by the spatial change in the magnetic field. The flux profile within the slab is calculated using Ampère's law $dh/dx=(4\pi/c)J$ and assuming a certain relationship between $J(x)$ and $h(x)$. Various models have been proposed for this relationship. For example, in the original Bean model, J is independent of h, and one obtains linear flux profiles. In the Kim-Anderson model, J is inversely proportional to h. This yields nonlinear flux profiles which are illustrated by the solid lines in Fig. 1(a). As a measure for the variation of the local field within the slab, we define Δ^* as the difference between the field at the surface and the field in the middle of the slab. In the original Bean model, Δ^* is a constant H^*. In general, Δ^* decreases as the external field H is increased, because J is always a monotonically decreasing function of h. For example, in the Kim-Anderson model, $\Delta^*=H[1-\sqrt{1-(H_p/H)^2}]$, where H_p is the smallest field that penetrates the whole sample. (See Appendix A.)

In any model, when the applied field H is much larger than Δ^*, the variations of the local field h are very small compared to the field at the surface. Hence $J(h)$ can be approximated by $J(H)$, yielding linear flux profiles with a slope $S=4\pi J(H)/c$ [upper solid line in Fig. 1(a)]. When H is not high enough to linearize the whole flux profile, one can still approximate the flux profile near the surface by straight lines with the slope S [dashed lines in Fig. 1(a)].

Let us now assume that H is decreased from H_{max} by a small amount ΔH. If H is of the same order of Δ^*, then the flux profiles are nonlinear. However, the condition $\Delta H \ll H$ implies $\Delta H \ll \Delta^*$; hence, the flux profile changes only near the surface, where it is linear [dotted line in Fig. 1(b)]. If $H \gg \Delta^*$, then the whole profile is approximately linear, and ΔH may be larger than Δ^* [dot-dashed line in Fig. 1(b)]. We conclude that in both cases the *variation* of the magnetization can be calculated assuming linear profiles with a slope $S=4\pi J(H)/c$.

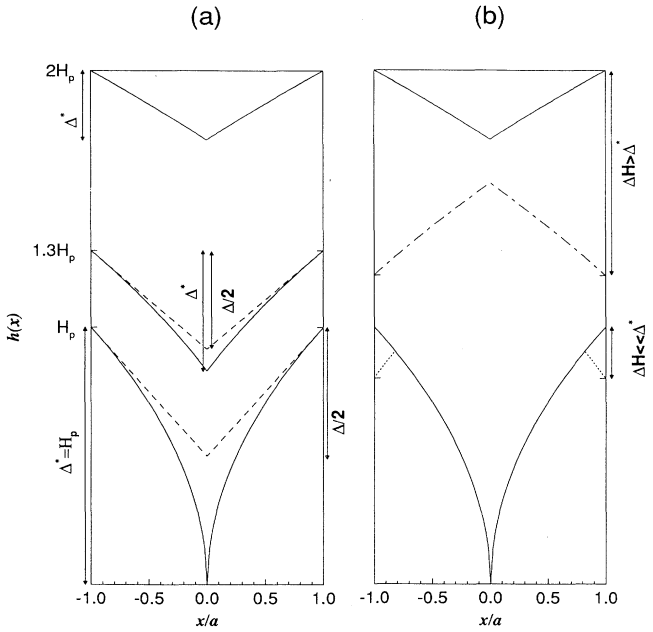

FIG. 1. Magnetic flux profiles in superconducting slab calculated on basis of Kim-Anderson model (a) in a steady field H and (b) after H is reduced by ΔH. Note that the curves for $H \geq 2H_p$ are already linear and that for the nonlinear profile changes occur only near the surface, where it is linear.

The magnetization induced when the field H is cycled between H_{max} and H_{min} can now be calculated in terms of $\Delta=2Sa$, where $2a$ is the width of the slab. When H is decreasing from H_{max} by $\Delta H=H_{max}-H<\Delta$, the magnetization is

$$M(\Delta H<\Delta)=M(H_{max})+\Delta H\left[1-\frac{\Delta H}{4\Delta}\right] . \tag{1}$$

When $\Delta H \geq \Delta$ the magnetization is proportional to the area of the triangle indicated by a dot-dashed line in Fig. 1(b) and it is independent of ΔH:

$$M(\Delta H>\Delta)=M(H_{min}) . \tag{2}$$

Similarly, when H is increasing from H_{min} by $\Delta H=H-H_{min}$,

$$M(\Delta H<\Delta)=M(H_{min})-\Delta H\left[1-\frac{\Delta H}{4\Delta}\right] \tag{3}$$

and

$$M(\Delta H>\Delta)=M(H_{max}) . \tag{4}$$

The corresponding expressions for $H(t)=H_{dc}+H_{ac}\sin(\omega t)$ are as follows: For decreasing $H(t)$,

$$M\left[\frac{\pi}{2}<\omega t<\frac{3\pi}{2}\right]=\begin{cases} M(H_{max})+H_{ac}[(1-\sin\omega t)-\frac{1}{4}\delta(1-\sin\omega t)^2] , & \sin\omega t \geq 1-2/\delta \\ M(H_{min}) , & \text{otherwise} , \end{cases} \tag{5}$$

and for increasing $H(t)$,

$$M\left[\frac{3\pi}{2}<\omega t<\frac{5\pi}{2}\right]=\begin{cases}M(H_{\min})-H_{ac}[(1+\sin\omega t)-\frac{1}{4}\delta(1+\sin\omega t)^2]\ , & \sin\omega t\le 2/\delta-1\\ M(H_{\max})\ , & \text{otherwise}\ .\end{cases} \tag{6}$$

Here we have introduced a parameter $\delta=H_{ac}/Sa=2H_{ac}/\Delta$ which may be viewed as a measure for the extent of penetration of the alternating field into the slab. In the original Bean model, $\delta=H_{ac}/H^*$, and in the Anderson-Kim model, $\delta=2H_{ac}H_{dc}/H_p^2$. The derivation of these expressions as well as additional expressions for δ in other models are given in Appendix A.

Based on Eqs. (5) and (6), the in-phase and out-of-phase harmonic susceptibilities χ_n' and χ_n'', respectively, can be calculated:

$$\chi_n'=\frac{1}{\pi H_{ac}}\int_0^{2\pi}M(t)\sin(n\omega t)d(\omega t)\ , \tag{7}$$

$$\chi_n''=\frac{-1}{\pi H_{ac}}\int_0^{2\pi}M(t)\cos(n\omega t)d(\omega t)\ . \tag{8}$$

In these expressions the magnetization [Eqs. (5) and (6)] is normalized by H_{ac}; therefore, the only parameter left after integration over one cycle is δ. This result implies that the harmonic susceptibilities depend on a single parameter δ, which measures the extent of penetration of the ac field into the slab. Hence the harmonic susceptibilities as a function of any experimental variable (e.g., ac field, dc field, temperature, and dimensions) can be reduced to universal curves, which describe the harmonic susceptibilities versus δ. Consequently, the maximum values which can be attained by the harmonic susceptibilities as a function of experimental variables are universal constants (as calculated below).

The integrals (7) and (8) can be performed analytically. Expressions for the harmonic susceptibility up to $n=7$ are given in Table I. Table II lists the peak values and positions of the harmonic susceptibilities for $n=3$, 5, and 7. General expressions for χ_n' and χ_n'' are derived in Appendix B. Plots of χ_n' and χ_n'' as a function of δ are shown in Fig. 2 for $n=1$, 3, 5, and 7. These curves also describe χ_n' and χ_n'' versus H_{ac}, since in any model δ is proportional to H_{ac}. In the Kim-Anderson model, δ is linearly dependent on H_{dc} as well. Therefore, in this specific model, the curves of Fig. 3 also describe the dependence of χ_n' and χ_n'' on H_{dc}. The parameter δ may also be changed by varying the temperature. The "deformation" of the δ scale depends on two relationships: first, the specific relationship between δ and physical parameters that may vary with temperature (e.g., H_p), and second, the dependence of these parameters on temperature. As an example, Fig. 3 shows $|\chi_3|$ versus temperature in the Kim-Anderson model for three H_{dc} values, assuming[2]

$$H_p(T)=H_p(0)[1-(T/T_c)^2]\sqrt{1-(T/T_c)^4}\ .$$

The salient features of these curves, i.e., the shift and broadening of the peaks and the invariance of the peak values, have been observed in many experiments.[1,3] Fitting of such theoretical curves to experimental data may help in deciding which model is suitable for a specific material. In the next section we illustrate this process using experimental data taken in a polycrystalline sample of YBCO.

TABLE I. Expressions for χ_n.

n		$\delta<1$	$\delta>1$
1	χ'	$-1+\frac{\delta}{2}$	$(\delta/2-1)(\alpha/\pi-\frac{1}{2})+(\delta/2+2/3\delta-\frac{2}{3})\cos\alpha/\pi$
			$\alpha=\sin^{-1}(1-2/\delta)\ ,\quad \pi/2\le\alpha\le 3\pi/2$
	χ''	$\frac{2\delta}{3\pi}$	$\frac{2}{3\pi\delta}(3-2/\delta)$
3	χ'	0	$-32(1-1/\delta)^{5/2}/15\pi\delta^{3/2}$
	χ''	$\frac{2\delta}{15\pi}$	$2(16/\delta^3-40/\delta^2+30/\delta-5)/15\pi\delta$
	$\lvert\chi\rvert$	$\frac{2\delta}{15\pi}$	$2(20/\delta^2-44/\delta+25)^{1/2}/15\pi\delta$
5	χ'	0	$32(1-1/\delta)^{5/2}(32/\delta^2-32/\delta+5)/105\pi\delta^{3/2}$
	χ''	$\frac{2\delta}{105\pi}$	$-2(512/\delta^5-1792/\delta^4+2352/\delta^3-1400/\delta^2+350/\delta-21)/105\pi\delta$
	$\lvert\chi\rvert$	$\frac{2\delta}{105\pi}$	$2(896/\delta^4-3072/\delta^3+3892/\delta^2-2156/\delta+441)/105\pi\delta^{1/2}$
7	χ'	0	$-32(1-1/\delta)^{5/2}(640/\delta^4-1280/\delta^3+880/\delta^2-240/\delta+21)/315\pi\delta^{3/2}$
	χ''	$\frac{2\delta}{315\pi}$	$\frac{2}{315\pi\delta}\left[\frac{10240}{\delta^7}-\frac{46080}{\delta^6}+\frac{84480}{\delta^5}-\frac{80640}{\delta^4}+\frac{42336}{\delta^3}-\frac{11760}{\delta^2}+\frac{1470}{\delta}-45\right]$
	$\lvert\chi\rvert$	$\frac{2\delta}{315\pi}$	$\frac{2}{315\pi\delta}\left[\frac{19200}{\delta^6}-\frac{85760}{\delta^5}+\frac{155520}{\delta^4}-\frac{145920}{\delta^3}+\frac{74340}{\delta^2}-\frac{19404}{\delta}+2025\right]^{1/2}$

TABLE II. Extrema values of χ_n (SI).

n	χ'		χ''		$\lvert\chi\rvert$	
	δ	χ	δ	χ	δ	χ
3	2.7	−0.048	1.4	0.056	1.7	0.061
			9.6	−0.10		
	1.2	0.0023	1.1	−0.0066	1.1	0.0067
5	2.1	−0.0062	1.5	−0.0017	1.5	0.0018
	6.9	0.011	3.3	−0.15	3.7	0.17
			26.0	0.0022		
	1.1	−0.0004	1.0	0.0021	1.0	0.0021
	1.4	0.0011	1.2	0.0012	1.2	0.0012
7	2.0	−0.0020	1.7	0.0036	1.7	0.0036
	3.8	0.0030	2.7	−0.0004	2.6	0.0004
	13.0	−0.0041	6.3	0.0058	8.8	0.0058
			51.0	−0.0008		

ANALYSIS OF EXPERIMENTAL RESULTS

Figure 4 describes measurements of the third-harmonic signal $|V_3|$ in a slab of a sintered YBCO ($1\times5\times7.4$ mm^3). The measurements were performed as a function of temperature in various dc fields applied parallel to the long dimension. A constant ac field of amplitude 43 mOe and frequency 20 kHz was applied in the same direction. As predicted by our analysis, the width and peak position of these curves vary with the applied dc field, while the peak values remain the same. As an illustration, we fit these data to our theoretical model and in the process we decide upon a suitable model for the critical current versus field and temperature.

First, $\delta(T,H_{dc})$ is found by the following method: Each curve is normalized relative to its peak value, and the temperature T_{peak} of the peak is found. Then, using Tables I and II, having in mind that $T>T_{peak}$ corresponds to $\delta>\delta_{peak}$, δ is calculated linearly (if $T<T_{peak}$ and $V_3/V_{3\,max}<\chi_3/\chi_{3\,max}$) or by numerically solving a transcendental equation (otherwise). The extracted values of δ versus field and temperature are shown in Fig. 5 (discrete points). Second, a suitable model for the relationship between J and h is chosen. The very strong and sharp dependence of δ upon T (and, for fixed T, upon H_{dc}) suggests the exponential model[9] (see Appendix A). Therefore, we assume

$$\delta(T)=P(T)\exp\left[\frac{A}{[1-(T/T_i)^2]^\gamma}\right], \tag{9}$$

where

$$P(T)=\frac{p_0}{1-(T/T_c)^2} \tag{10}$$

varies slowly with temperature.

To find T_i and A, we take only values of $\delta>5$, where $P(T)$ can presumably be neglected relative to the ex-

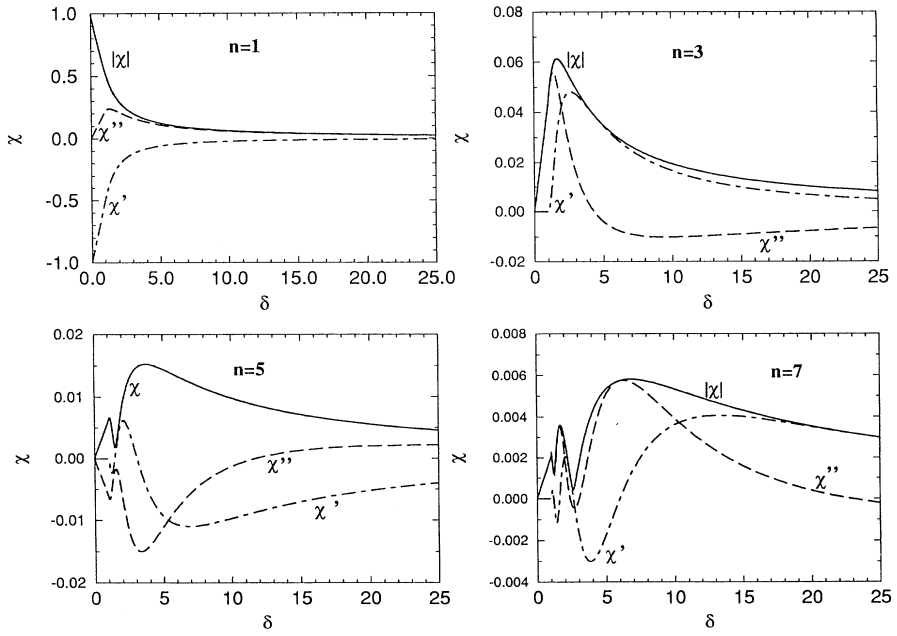

FIG. 2. Calculated universal curves describing harmonic susceptibilities vs δ.

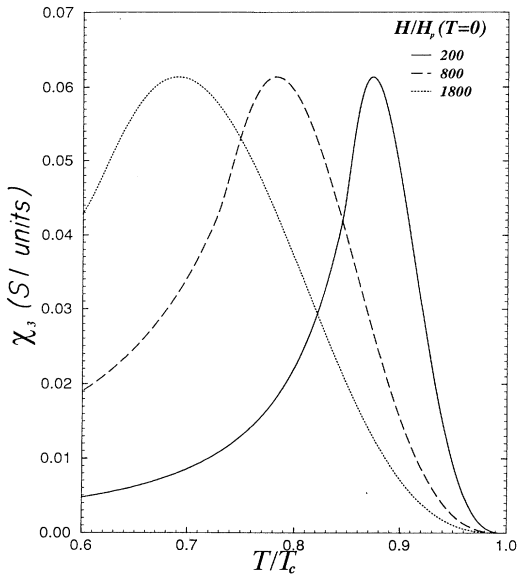

FIG. 3. Calculated curves of $|\chi_3|$ vs temperature for various external steady fields (normalized).

ponential term. This enables a linear least-squares fit:

$$(\ln\delta_n)^{-1/\gamma} = A^{-1/\gamma} - \frac{A^{-1/\gamma}}{T_i^2} T_n^2 \ . \tag{11}$$

The value $\gamma = 2$ was found to give the best fit. Knowing T_i and A, a fit to $P(T)$ is found, using a similar method as above. Here values of $\delta > 0.5$ were used to resolve the dependence where the exponential is not dominant (values of $\delta < 0.5$ were omitted, because the data were not smooth enough).

Values of the four parameters A, p_0, T_i, and T_c, for each H_{dc} curve, are given in Table III. Taking into account the statistical errors in A and p_0 (about 10%), Fig. 6 indicates that the coefficients A and p_0 increase with H_{dc}, approximately linearly. The model emerging from our analysis is that the pinning force is a function of temperature and field:

$$\alpha = \alpha_0(T) \exp\left[-\frac{H_{dc}}{H_0(T)} \right] , \tag{12}$$

where

$$\alpha_0(T) = \alpha_0(0)\left[1 - \left[\frac{T}{T_c} \right]^2 \right] \tag{13}$$

and

$$H_0(T) = H_0(0)\left[1 - \left[\frac{T}{T_i} \right]^2 \right]^2 . \tag{14}$$

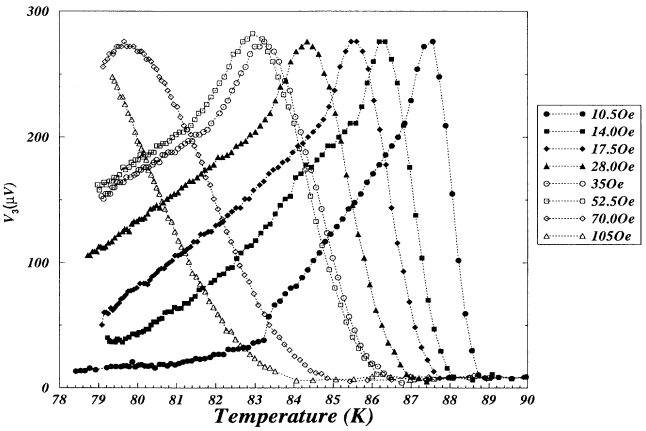

FIG. 4. Third-harmonic signal vs temperature measured in slab of sintered YBCO in various dc fields.

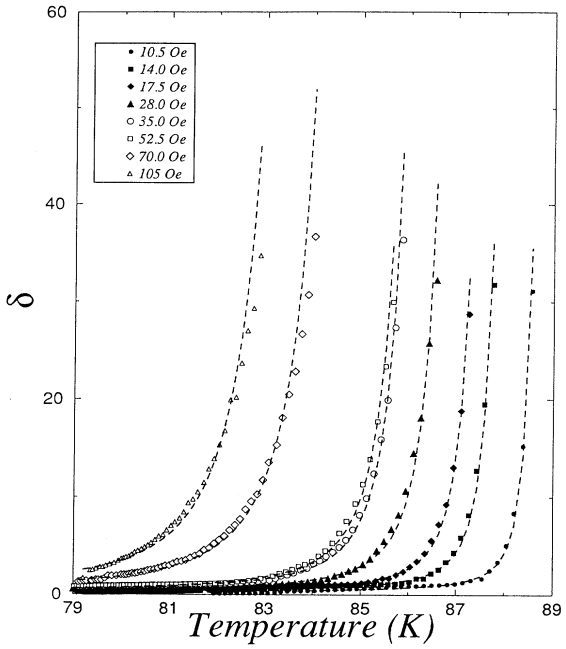

FIG. 5. Extracted values of δ vs temperature for various dc fields (discrete points) and theoretical fits (dashed lines) to Eqs. (9) and (10).

The Kim-Anderson model assumes a constant pinning force which may depend upon T, but not upon H. The exponential dependence upon H comes from the exponential model.[9] However, the latter makes assumptions about the critical current itself, not about the pinning force. Therefore the model emerging from our

TABLE III. Parameters used in the fits of Fig. 5.

H_{dc} (Oe)	A	p_0	T_i (K)	T_c (K)
10.5	2.1×10^{-3}	6.0×10^{-2}	89.7	91.2
14.0	4.4×10^{-3}	7.2×10^{-2}	89.3	91.0
17.5	6.1×10^{-3}	7.3×10^{-2}	89.2	90.4
28.0	1.0×10^{-2}	8.7×10^{-2}	88.9	90.3
35.0	1.2×10^{-2}	0.11	88.4	90.8
52.5	1.4×10^{-2}	0.11	88.5	90.4
70.0	3.1×10^{-2}	0.14	88.1	89.3
105.0	3.9×10^{-2}	0.18	87.5	90.2

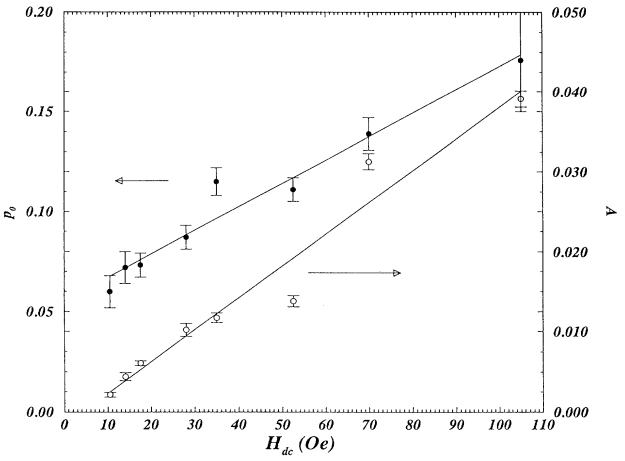

FIG. 6. Extracted values of A and p_0 [Eqs. (9) and (10)] vs H_{dc}. Solid lines represent the best linear fits.

straightforward data analysis is a combination of these two models.

The numerical values obtained for the two constants of the model are $H_0(0)=2500\pm200$ Oe and $\alpha_0(0)=29\pm2.5$ COe cm^{-3}. We note that in this model the parameters T_c and T_i have the meaning of the transition temperature and the irreversibility temperature,[10] respectively. This physical meaning becomes apparent from the above expressions for α_0 and $\alpha(T)$. The preexponential coefficient $\alpha_0(T)$, and consequently the critical current J, vanishes at T_c even when $H=0$. The exponential part of α vanishes at any temperature if H_0 vanishes, when even the smallest external field H is applied. The statistical errors in A and p_0 do not allow us to determine T_i and T_c with high accuracy. However, within the error margins, (T_c-T_i) is positive and in general increases with H_{dc}, as expected.

The values of δ, as calculated from the above fit, are shown in Fig. 5 by dashed lines. Once δ is calculated for each T, the universal curve is formed by plotting the measured $|V_3|$ versus δ, as calculated from the parameters of Table III, and the measured temperature. Figure 7 demonstrates the universality of the curves for any scale of δ.

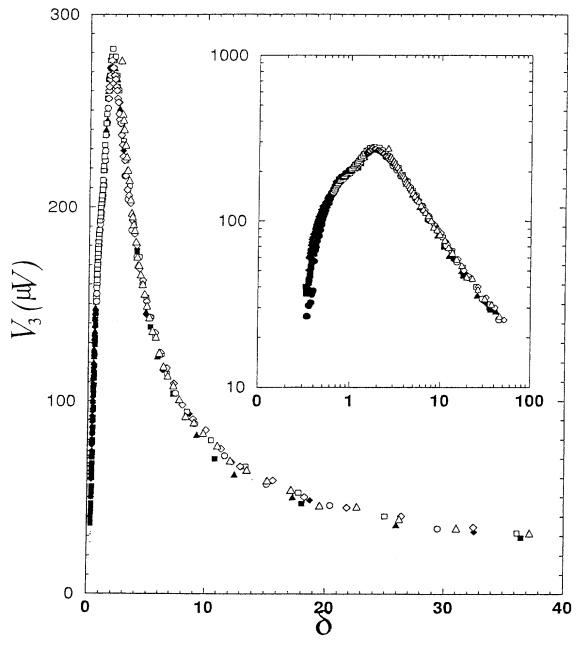

FIG. 7. Universal curve formed by plotting data of Fig. 4 vs δ in linear and logarithmic (inset) scales.

DISCUSSION

We have analyzed the alternating magnetic response of type-II superconductors on the basis of the critical-state theory, assuming a small applied alternating field which probes the magnetic state of the sample. The alternating response is a function of several experimental variables, e.g., the amplitude of the alternating field, the steady bias field, temperature, and dimensions of the sample. Experimentally, only one variable is changed while all the other are kept constant. A variety of such experiments has been performed in high-temperature superconductors varying the temperature,[3] the amplitude of the alternating field,[11–13] the steady bias field,[5] and the dimensions of the sample.[14] Our analysis shows that all these measurements are basically the same, as they all can be reduced to universal curves which describe the harmonic susceptibilities as a function of the parameter δ. Moreover, our analysis shows that in such measurements a peak always appears, and it always has the same value, regardless of the physical parameter that varies in the measurement. For example, the peak value reached in measurements of the third-harmonic susceptibility $|\chi_3|$ as a function of temperature should be the same as the peak value reached in measurements of $|\chi_3|$ as a function of the steady bias field. In either case, the value of $\delta\cong1.7$, which corresponds to the peak of $|\chi_3|$, is achieved by changing the steady bias field or temperature. Our analysis also predicts that the peak values of the harmonic susceptibilities are the same for all type-II superconductors for which the critical-state theory is valid.

The magnitude of the harmonic susceptibilities rises as δ and falls as $1/\delta$; hence, the mathematical explanation for the existence of peaks is clear. The physical origin of the peaks may be understood considering the ratio between the amplitude of the alternating field and the difference between the local fields in the middle and at the surface of the sample. When this ratio is small, the alternating field does not penetrate much into the sample; the whole signal is small and so are its harmonics. Any increase of this ratio will result in a larger signal; however, beyond a certain point, the alternating field penetrates the whole sample and the signal attains its maximum possible value. Any further increase of the ratio will not change the signal, but the resulting normalized harmonics (relative to H_{ac}) will be smaller.

Our analysis assumes that volume pinning dominates and neglects surface barrier effects. The opposite extreme case, where surface currents dominate, was discussed by Gilchrist and Konczykowski.[15] Their analysis also predicts a peaked behavior of the harmonics. Simi-

larly to our parameter δ, they define a parameter j and express the harmonics in terms of it. The details of their results are different from ours, because they studied current loops and not a slab. However, the ability to describe the behavior of the harmonics in terms of a single parameter and to produce the peaks are common features of both analyses.

The critical-state model, on which our analysis is based, assumes that the magnetic response of the material is independent of the frequency of the applied alternating field. Our analysis may be extended by taking into account the dynamics of flux motion within the sample. The parameter δ may still be defined, although its value may depend on the frequency of the alternating field. Clearly, the frequency dependence will introduce an additional parameter to the model. However, for a fixed frequency the qualitative observations of our analysis will remain valid.

We have illustrated the application of our analysis by analyzing one example of experimental data taken in a sintered YBCO sample. Clearly, more analyses of experimental data are necessary to demonstrate the validity of our results. Beside demonstrating the universality of the alternating magnetic response, such analyses will provide models for the dependence of the critical current density upon field and temperature.

ACKNOWLEDGMENTS

We thank the National Council for Research and Development for partial support of this work.

APPENDIX A: CALCULATION OF THE PARAMETER δ IN VARIOUS MODELS

1. Bean model

In the original Bean model, a constant J_c is assumed. Therefore

$$H^*=4\pi a J_c/c \ , \tag{A1}$$

$$\Delta=2\Delta^*=2H^* \ , \tag{A2}$$

and

$$\delta=H_{ac}/H^* \ . \tag{A3}$$

2. Kim-Anderson model

This model assumes a constant pinning force α, which balances the driving force acting on the flux vortices: $\bar{F}=\bar{J}\times\bar{h}/c=\bar{\alpha}$. The full penetration field H_p depends on the slab dimension a and on the pinning force α: $H_p=\sqrt{8\pi\alpha a}$. The local field is

$$h(x)=\sqrt{\pm H_p^2(x/a-1)+H^2} \ , \tag{A4}$$

where the plus and minus signs relate to increasing or decreasing external field, respectively.

The maximum field variation is

$$\Delta^*=H-h(0)=H[\pm1\mp\sqrt{1\mp(H_p/H)^2}] \ . \tag{A5}$$

When $H_{max}=H_p$ the nonlinearity of $h(x)$ is apparent (see Fig. 1). However, the curves for $H>H_p$ are nearly linear with a slope

$$S(x)=H_p^2/2ah(x)\cong H_p^2/2aH \ . \tag{A6}$$

In this linear limit,

$$\Delta^*\approx H_p^2/2H_{dc} \ , \tag{A7}$$

$$\Delta=H_p^2/H_{dc} \ , \tag{A8}$$

and

$$\delta=2H_{ac}H_{dc}/H_p^2 \ , \tag{A9}$$

where H has been replaced by H_{dc}, assuming $H_{ac}\ll H_{dc}$.

Consider the case $H\approx H_p$ (nonlinear field profile). If H_{ac} is small enough, the variation of $H(t)$ influences only the region near the surface, where the slope is a constant. The general criterion for local linearity is $J(H_{max})\approx J(H_{min})$. In the Kim-Anderson model, where J is inversely proportional to H, this condition is equivalent to the condition $H_{min}\approx H_{max}$, i.e., $H_{ac}\ll H_{dc}$. This means that the above δ can be used in all the expressions for χ, even in the highly nonlinear cases, as long as $H_{ac}\ll H_{dc}$.

3. Power-law model

The pinning force here is some (fractional) power of the local field:

$$\alpha_c=\alpha_0(h/H_0)^\gamma \ . \tag{A10}$$

For $\gamma=1$, the pinning force is linear in h; therefore, J_c is constant and one obtains the Bean model. The Kim-Anderson model is obtained with $\gamma=0$. Therefore we write below only the final results. The derivation and argumentation are the same as in the above model. The full penetration field is

$$H_p=[4\pi(2-\gamma)\alpha_0 a/H_0^\gamma]^{1/(2-\gamma)} \ , \tag{A11}$$

the local field is

$$h(x)=[\pm H_p^{2-\gamma}(x/a-1)+H^{2-\gamma}]^{1/(2-\gamma)} \ , \tag{A12}$$

and the maximum field variation is

$$\Delta^*=H-h(0)=H\{\pm1\mp[1\mp(H_p/H)^{2-\gamma}]^{1/(2-\gamma)}\} \ . \tag{A13}$$

In the linear limit,

$$\Delta=2/(2-\gamma)H_p^{2-\gamma}/H_p^{1-\gamma}$$

and

$$\delta=(2-\gamma)H_{ac}H_{dc}^{1-\gamma}/H_p^{2-\gamma} \ .$$

4. Exponential model

The exponential model assumes

$$J(h)=J_0\exp(-h/H_0) \ . \tag{A14}$$

The linearity condition can be evaluated directly:

$$J(H_{min})/J(H_{max})=\exp[(H_{max}-H_{min})/H_0]$$
$$=\exp(2H_{ac}/H_0)\cong1 \ . \tag{A15}$$

Hence $H_{ac} \ll H_0$ is a sufficient condition, and there is no restriction on H_{dc} (which may approach zero).

Field-profiles are given by

$$h(x)=H_0\ln[\pm(4\pi/c)(J_0a/H_0)(x/a-1)+\exp(H/H_0)] , \tag{A16}$$

where the plus and minus signs refer to ascending and descending branches, respectively. Substituting $H=H_p$ and $h(x=0)=0$, we get

$$H_p=H_0\ln(4\pi J_0a/cH_0+1) . \tag{A17}$$

The maximum field variation is

$$\Delta^*=\mp H_0\ln[1\mp(\exp H_p/H_0-1)\exp(-H/H_0)] . \tag{A18}$$

When $H \gg H_0$, the constant term in Eq. (A15) is much larger than the varying one, and so the ln function can be expanded to the first order in x/a, which yields a linear flux profile. However, the linearized model is valid for any value of H_{dc}, as indicated above.

Taking $H_{ac} \ll H_{dc}$, Δ is determined by $J(H)$:

$$\Delta=2H_0(\exp H_p/H_0-1)\exp(-H_{dc}/H_0) , \tag{A19}$$

and

$$\delta=H_{ac}\exp(H_{dc}/H_0)/H_0(\exp H_p/H_0-1) . \tag{A20}$$

APPENDIX B: DERIVATION OF GENERAL EXPRESSIONS FOR χ_n

The integration (7) and (8) yields:

$$\chi_n'=\{[(n^2-4)(n^2+1)\sin^2x_0+n^2(n^2-1)\cos^2x_0-(n^2-1)(n^2-2)]\cos nx_0 + 6n\cos x_0\sin nx_0\}/2\pi(\sin x_0-1)n(n^2-4)(n^2-1) , \tag{B1}$$

$$\chi_n''=\{2(-1)^{(n-1)/2}(n^2-4)\sin x_0-2(-1)^{(n-1)/2}(n^2-1) +[-(n^2-4)(n^2+1)\sin^2x_0-n(n^2-1)\cos^2x_0+(n^2-1)(n^2-2)]\sin nx_0 + 6n\cos x_0\sin x_0\cos nx_0\}/2\pi(1-\sin x_0)n(n^2-4)(n^2-1) , \tag{B2}$$

where

$$\sin x_0=1-2/\delta . \tag{B3}$$

These expressions are similar to those derived by Ji *et al.*[2] They can be related to the Tchebychev polynomials

$$T_n(c)=\cos(n\cos^{-1}c) , \quad U_n(c)=\sin[(n+1)\cos^{-1}c]/\sin(\cos^{-1}c) . \tag{B4}$$

In our case,

$$c\equiv\cos x_0=\sqrt{4/\delta(1-1/\delta)} , \tag{B5}$$

$$s\equiv\sin x_0=1-2/\delta . \tag{B6}$$

It follows from Eq. (B3) that

$$U_{n-1}^2(c)=[1-T_n^2(c)]/s^2 . \tag{B7}$$

Using Eqs. (B3)–(B6) yields

$$\chi_n'=\{U_{n-1}(c)6cn(1-c^2)+T_n(c)(2n^2c^2-6+4c^2)\}/\pi n(n^2-1)(n^2-4)(s-1) , \tag{B8}$$

$$\chi_n''=\{U_{n-1}(c)s(2n^2c^2-6+4c^2)+T_n(c)6scn+(-1)^{(n-1)/2}(8s-2n^2s-2+2n^2)\}/\pi n(n^2-1)(n^2-4)(s-1) , \tag{B9}$$

$$|\chi_n|=(U_{n-1}(c)(-1)^{(n-1)/2}\{8(n^2-4)(n^2+2)c^4+8[s(n^2+2)(n^2-1)-(n^2-4)(n^2+5)]c^2-24[s(n^2-1)+4-n^2]\} + T_n(c)(-1)^{(n-1)/2}[-24n(n^2-4)c^3-24n(4-s+sn^2-n^2)c]+4(n^2-4)(n^2-1)c^4+4(n^2-4)(n^2-7)c^2 - 8(n^2-4)(n^2-1)s+104-40n^2+8n^4)^{1/2}/\pi n(n^2-4)(n^2-1)(s-1) . \tag{B10}$$

The explicit form of the Tchebychev polynomials is

$$T_n(c)=nc(-1)^N\sum_{j=0}^{N}(-1)^j\frac{(N+j)!2^{2j+1}}{(N-j)!(2j+1)!}c^{2j} , \tag{B11}$$

$$U_{n-1}(c)=c(-1)^N\sum_{j=0}^{N}(-1)^j\frac{(N+j)!2^{2j+1}}{(N-j)!(2j)!}c^{2j} , \tag{B12}$$

where

$$N=\frac{n-1}{2} . \tag{B13}$$

Using Eqs. (B11) and (B12), collecting terms of c, and substituting Eqs. (B4) and (B5), we get

$$\chi_n'=\frac{(-1)^N\delta^{-3/2}}{\pi}\left[1-\frac{1}{\delta}\right]^{5/2}\left[(-1)^{N+1}\frac{2^{2n+1}(1-1/\delta)^{N-1}}{n(n+1)(n+2)}+\sum_{j=1}^{N}\frac{(-1)^{j+1}2^{4(j+1)}j(n+1-2j)(N+1+j)!\delta^{1-j}(1-1/\delta)^{j-1}}{(n+1+2j)(2j+3)(2j+1)(2j)!(N+1-j)!(n^2-1)}\right], \tag{B14}$$

$$\chi_n''=\frac{(-1)^N\delta^{-1}}{\pi}\left\{2\frac{3-2/\delta}{n(n^2-4)}+\left[1-\frac{1}{\delta}\right]\left[1-\frac{2}{\delta}\right]\times\left[(-1)^{N+1}\frac{2^{2n}\delta^{1-N}}{n(n+1)(n+2)}+\sum_{j=1}^{N-1}\frac{(-1)^j2^{4j+1}(2j-1)(n+1-2j)(N+1+j)!\delta^{1-j}(1-1/\delta)^j}{(n+1+2j)(j+1)(2j)!(N+1-j)!(n^2-4)}\right]\right\}, \tag{B15}$$

and

$$|\chi_n|=\frac{\delta^{-1}}{\pi}\left\{4\frac{12/\delta^3-34/\delta^2+28/\delta-5}{n^2(n^2-4)^2}+\left[1-\frac{1}{\delta}\right]^2\left[\frac{4}{3}\frac{2n^2(23-20/\delta)-4n^2(1-1/\delta)}{n^2(n^2-4)^2}+(-1)^N\frac{2^{2n+3}\delta^{2-N}}{n(n+1)(n+2)}\left[1-\frac{1}{\delta}\right]^N+(-1)^{N-1}\frac{2^{2n-1}\delta^{3-N}(n+1)(n-1)^2/\delta+n^4-3n^3-8n^2+28}{n^2(n-2)(n-1)^2(n+2)^2}\left[1-\frac{1}{\delta}\right]^{N-1}+\left[1-\frac{1}{\delta}\right]^2\sum_{j=2}^{N-2}\frac{(-1)^j2^{4j+3}(n+1-2j)(N+1+j)!\delta^{2-j}(1-1/\delta)^{j-2}}{(n+1+2j)(j+1)(2j)!(N+1-j)!(n^2-4)}A_j\right]\right\}^{1/2}, \tag{B16}$$

where

$$A_j=(n^2-1)(n+1+2j)(n-1-2j)/\delta+(4j^2+6j-7)n^2-4j^2-12j+19 . \tag{B17}$$

The above formulas are quite detailed and are given here for the sake of completeness. Nevertheless, several properties can be deduced from these general expressions.

(1) The harmonic susceptibilities and their components are polynomials of δ. The in-phase components have in addition two factors of fractional power. In the limits $\delta=1$ and $\delta=\infty$, the behavior is

$$\chi_n'(1)=0 , \quad \chi_n'(\delta\to\infty)=\frac{32}{15\pi}(-1)^N\delta^{-3/2} , \tag{B18}$$

$$\chi_n''(1)=(-1)^N\frac{-2}{\pi n(n^2-4)} , \quad \chi_n''(\delta\to\infty)=\frac{2}{\pi n}(-1)^N\delta^{-1} , \tag{B19}$$

$$|\chi_n|(1)=\frac{2}{\pi n(n^2-4)} , \quad |\chi_n|(\delta\to\infty)=\frac{2}{\pi n\delta} . \tag{B20}$$

(2) All the even harmonics vanish.

(3) For $\delta<1$, all out-of-phase components of n (odd) >1 are proportional to δ and all in-phase components vanish.

(4) For $\delta\gg1$, all out-of-phase components decay as δ^{-1}, and all in-phase components decay as $\delta^{-3/2}$.

(5) All odd harmonics for $n>1$ have at least one peak. The out-of-phase components have $n-1$ extreme points, half of them maxima and the other half minima. The in-phase components and also the absolute values have $n-2$ extreme points, of which $(n-1)/2$ are maxima and $(n-3)/2$ are minima.

*On leave from Philips Laboratories, North American Philips Corporation, Briarcliff-Manor, New York 10510.

[1]A. Shaulov and D. Dorman, Appl. Phys. Lett. **53**, 2680 (1988).
[2]L. Ji, R. H. Sohn, G. C. Spalding, C. J. Lobb, and M. Tinkham, Phys. Rev. B **40**, 10 936 (1989).
[3]T. Ishida and R. B. Goldfarb, Phys. Rev. B **41**, 8937 (1990).
[4]D. G. Xenikos and T. R. Lemberger, Phys. Rev. B **41**, 869 (1990).
[5]A. Shaulov, Y. Yeshurun, S. Shatz, R. Hareuveni, Y. Wolfus, and S. Reich, Phys. Rev. B **43**, 3760 (1991).
[6]C. P. Bean, Rev. Mod. Phys. **36**, 31 (1964).
[7]T. Ishida and H. Mazaki, J. Appl. Phys. **52**, 6798 (1981).
[8]C. Jeffries, Q. H. Lam, Y. Kim, L. C. Bourne, and A. Zettl, Phys. Rev. B **37**, 9840 (1988); C. D. Jeffries, Q. H. Lam, Y. Kim, C. M. Kim, A. Zettl, and M. P. Klein, *ibid.* **39**, 11 526 (1989).
[9]G. Ravi Kumar and P. Chaddah, Phys. Rev. B **39**, 4704 (1989).
[10]A. P. Malozemoff, T. K. Worhington, Y. Yeshurun, F. Holtzberg, and P. Kes, Phys. Rev. B **38**, 7203 (1988).
[11]S. D. Murphy, K. Renouard, R. Crittenden, and S. M. Bhagat, Solid State Commun. **69**, 367 (1989).
[12]L. Civale, T. K. Worhington, L. Krusin-Elbaum, and F. Holtzberg, in *Nonlinear AC Susceptibility Response Near the Irreversibility Line,* Proceedings of the Workshop on Magnetic Susceptibility of Superconductors and Other Spin Systems (S^4); Coolfont, West Virginia, 1991, edited by R. A. Hein, T. L. Francavilla, and D. H. Liebenberg (Plenum, New York, 1991).
[13]M. Sato, T. Kamimura, and T. Iwata, Jpn. J. Appl. Phys. **28**, 330 (1989).
[14]D. X. Chen, R. B. Goldfarb, J. Nogues, and K. V. Rao, J. Appl. Phys. **63**, 980 (1988).
[15]J. Gilchrist and M. Konczykowskii, Physica C **212**, 43 (1993).